RSC Advances

PAPER

View Article Online
View Journal | View Issue

Cite this: *RSC Adv.*, 2016, **6**, 105871

Synthesis of biocompatible polymeric nanomaterial dually loaded with paclitaxel and nitric oxide for anti-MDR cancer therapy†

Jing Fan,[ab] Jibin Song,[b] Yijing Liu,[b] Guocan Yu,[b] Ying Ma,[b] Yan Deng,[a] Nongyue He*[a] and Fuwu Zhang*[b]

Received 23rd September 2016
Accepted 22nd October 2016

DOI: 10.1039/c6ra23637e

www.rsc.org/advances

Nitric oxide (NO) as a chemosensitizer has attracted a lot of attention in anti-multidrug resistance (MDR) tumor therapy. In this study, a three-segment amphiphilic copolymer was synthesized through click reaction by azido and alkyne groups. The PEI part with abundant secondary amines was utilized to load NO gas molecules, the hydrophobic PLLA core to encapsulate the hydrophobic drug paclitaxel (PTX), and the mPEG shell to provide a hydrophilic interface and lead the copolymer to self-assemble into micelles in the water phase for biological applications. This multifunctional mPEG–PEI–PLLA–PTX–NO nanostructure is able to release NO spontaneously under physiological conditions and enhance the cytotoxicity for synergistic treatment of PTX and NO, demonstrating the potential to treat MDR tumors.

Introduction

With the extensive use of chemotherapeutics, multi-drug resistance (MDR) has become one of the main challenges for the successful clinical chemotherapy of cancer.[1] MDR in chemotherapy is thought to be caused by a two-hit mutation blocking of the drug target molecule and the activation of the second signaling pathway to excrete chemotherapeutics and maintain tumor growth. Some proteins and signal factors have been revealed to play roles in the tumor MDR process such as P-glycoprotein (P-gp), multidrug resistance-associated protein (MRP), lung resistance protein (LRP),[2] and breast cancer resistant protein (BCRP). Most of them belong to the ATP-binding cassette (ABC) transporter. The ABC transporter has been proven to be an important factor of the cell membrane which increases drug efflux.[3] The microenvironment changes of tumor tissues always lead to the decrease of chemosensitivity and glucose deprivation.[4] Then the generated low pH microenvironment in tumor would lead to the membrane permeability change for chemotherapeutic drugs.[5] On the other hand, drastic metabolism causes the hypoxic intra-tumor environment. There are evidences indicating that hypoxia in the intra-tumor environment also decreases the chemotherapeutic efficiency since some anticancer drugs require oxygen for activity.[6]

Nitric oxide (NO), a colorless, odorless, lipophilic and short-lived gas molecule, has been widely accepted as an important signal mediator in mammal's physiological process. It has been identified with important functions in cardiovascular system, central nervous system, mammal's early development, immune response, and anti-tumor effects.[7–11] It has been found that NO has the ability to reverse MDR and restore the chemosensitivity of tumor to chemotherapeutics.[12–16] It is generally recognized that NO reverses the chemosensitivity of tumor tissues through releasing oxidative stress. After ROS is reduced, the activation of scavenging and tolerance system of tumor cells such as the ABC transporter is inhibited and the outflow of chemotherapeutic drugs is prevented.[17–19] Recently, a light-responsive NO and doxorubicin release system based on degradable methoxy(polyethylene glycol)–poly(lactic-*co*-glycolic acid) (mPEG–PLGA) nanoparticle was developed. The NO was generated under the exposure of UV/Vis light, which broke the shell to release the localized DOX drug for anti-MDR therapy.[20]

The secondary amine of polyethylenimine (PEI) is an appropriate site to bind NO, which then serves as a NO donor with a spontaneous release capacity.[21,22] Nurhasni *et al.* reported that the naked PEI/NONOate donor had a short-life property with most of NO released in 2 h under physiological conditions. The poly(L-lactide) (PLLA) is a biocompatible and degradable organic aliphatic polyester.[23–25] It has been used as a biodegradable slow-release system for hydrophobic drugs which are

[a]*State Key Laboratory of Bioelectronics, Southeast University, Nanjing 210096, Jiangsu, P. R. China. E-mail: nyhe1958@163.com; fuwu.zhang@nih.gov*

[b]*Laboratory of Molecular Imaging and Nanomedicine (LOMIN), National Institute of Biomedical Imaging and Bioengineering (NIBIB), National Institutes of Health (NIH), Bethesda, MD 20892, USA*

† Electronic supplementary information (ESI) available: ^{1}H NMR spectrum of PEI–azide, ^{1}H NMR spectrum of PLLA–alkyne, ^{1}H NMR spectrum of mPEG–PEI–PLLA, HPLC chromatograph of mPEG–PEI–PLLA–PTX PBS solution, HPLC traces of different concentrations of PTX, PTX calibration curve, the release of PTX from mPEG–PEI–PLLA–PTX in PBS solution, Griess method analyzes NO loading and stability on mPEG–PEI–PLLA polymer, mPEG–PEI–PLLA–NO treated with UV exposure or sonication, UV-Vis spectrum of IR800 NIR dye before and after conjugation to the particles. See DOI: 10.1039/c6ra23637e

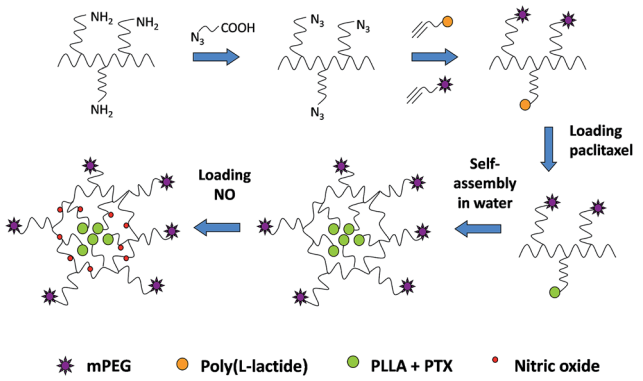

Fig. 1 The synthetic scheme of mPEG–PEI–PLLA–PTX–NO nanomedicine.

encapsulated through hydrophobic force. Methoxypoly (ethylene glycol) (mPEG) is a hydrophilic polymer which has been commonly used wrap around hydrophobic materials to improve water solubility and extend blood circulation time *in vivo*.[26,27]

In this research, a branched PEI was modified with 2-azidoacetic acid to introduce azido functional group. Then it reacted with alkyne-terminated mPEG and PLLA polymer *via* azide–alkyne Huisgen cycloaddition using copper bromide as the catalysts to afford a three-segment amphiphilic copolymer, where the hydrophobic part PLLA was used to encapsulate hydrophobic drugs while the secondary amine of PEI was to load nitric oxide. This multifunctional copolymer could be resuspended readily in water and self-assembled into micelle with a hydrophobic PLLA core and a hydrophilic PEG shell. After being loaded with first-line chemotherapeutic drug paclitaxel (PTX), the mPEG–PEI–PLLA–PTX–NO nanotherapeutics was shown to have higher cytotoxicity against OVCAR-8/ADR cancer cells over formulations that only contain either PTX or NO (Fig. 1).

Experimental section

Synthesis of PEI–azide

Branched PEI (MW = 10 000, Sigma-Aldrich) (100 mg) was mixed with 2-azidoacetic acid (CAS#18523-48-3, Sigma-Aldrich) (15 mg), and added 2-(1*H*-benzotriazol-1-yl)-1,1,3,3-tetramethyluronium hexafluorophosphate (HBTU, CAS#94790-37-1, Sigma-Aldrich) (303 mg), triethylamine (TEA, Sigma-Aldrich) (112 μL), dimethyl formamide (DMF, Sigma-Aldrich) (6 mL). After the amidation reaction between the amine group of PEI and carboxyl group of 2-azidoacetic acid overnight, the solution was kept in 6–8 kDa MWCO dialysis membrane and dialyzed in water. The dialysate was replaced for 5 times to remove the unreacted reagents. The purified product was freeze-dried and stored at −20 °C.

Synthesis of PLLA–alkyne

The 500 mg L-lactide (LA, Sigma-Aldrich) and 6.5 mg 2-propynyl alcohol (Sigma-Aldrich) were dissolved in 5 mL dichloromethane (DCM, Sigma-Aldrich). 1,8-Diazabicyclo[5.4.0]undec-7-ene (DBU, 26.4 mg, Sigma-Aldrich) was dissolved in 1.0 mL DCM and added into the above LA solution at room temperature. After stirring for 10 min, excess amount of acetic acid was added to quench the reaction and the solution was added dropwise into 40 mL hexane/diethyl ether (v/v = 2/1) to precipitate the target product. The reaction mixture was centrifuged at 9000 rpm for 5 min to remove the supernatant. The process was repeated 3 times for purification. Residual solvent was removed under vacuum. The obtained white powder was dissolved in $CDCl_3$ for ^{1}H-NMR characterization. Gel permeation chromatography (Waters 1515) was employed to characterize the molecular weight and the polydispersity index (PDI).

Synthesis of mPEG–PEI–PLLA

100 mg PEI–N_3 (MW = 11 500), 175 mg mPEG–alkyne (MW = 5000, Creative PEGWorks) and 150 mg PLLA–alkyne (MW = 4300) were dissolved in 7 mL DMF and degassed by N_2 for 30 min. Then 3 mg CuBr (Sigma-Aldrich) and 5 mg *N*,*N*,*N*′,*N*″,*N*″-pentamethyldiethylenetriamine (PMDETA, Sigma-Aldrich) were quickly added for click reaction in a sealed environment under N_2 protection. After stirring overnight, a 12 000–14 000 MW dialysis membrane (Spectra/Por) was utilized to remove unreacted materials (replenishing water for 5 times). The freeze-dried powder was characterized by ^{1}H-NMR in DMSO-D_6 solution and stored at −20 °C.

Conjugation of mPEG–PEI–PLLA with near-infrared fluorescent dye IR-800

In order to investigate the distribution of mPEG–PEI–PLLA micelle in cells and in mice, a near-infrared fluorescent dye IR-800 (IRDye® 800CW, LI-COR, Inc.) was conjugated to the positively charged mPEG–PEI–PLLA copolymer through amidation chemistry between primary amines of PEI and NHS ester of IR-800 for optical imaging.

The synthesized mPEG–PEI–PLLA (12 mg, about 0.4 μmol) was mixed with 0.5 mg of IR-800 dye (about 0.4 μmol) and dissolved in 5 mL DMF, 40 μL TEA was then added to the solution. After overnight stirring, mPEG–PEI–PLLA-IR-800 was purified by dialysis against pure water. The powder was obtained after lyophilization and stored in dark at −20 °C.

Fluorescence imaging of mPEG–PEI–PLLA-IR800 in multidrug resistant cell line OVCAR-8/ADR

In this study, all *in vitro* and *in vivo* experiments were performed in compliance with the NIH animal proposal (NIBIB 16-03) approved by the Animal Care and Use Committee (ACUC). OVCAR-8/ADR, a multidrug resistance ovarian tumor cell line, was seeded on a slide (Lab-Tek chamber slides, Thermo Scientific Nunc) at 5×10^4 density per well. The prepared mPEG–PEI–PLLA-IR800 (50 μg mL^{-1}) or free IR-800 solution (2 μg mL^{-1}) was placed on the slides. After incubation for 2 h, cells were washed with PBS to remove free micelles or free dye molecules. Then the slides were imaged under a fluorescence microscope (Olympus X81).

The nanoparticles conjugated with IR-800 were also tested in tumor mice. Ovcar-8/ADR cells (2×10^7/mouse) were inoculated in the right hind leg root of 5 week old female nude mice through subcutaneous injection. After 7 days of feeding, tumors with a size about 100 mm^3 were treated with about 100 μL of 50 μg mL^{-1} mPEG–PEI–PLLA-IR800, or 50 μg mL^{-1} mPEG–PEI–PLLA as the control group through intratumor injection. Then two groups of mice were imaged under small animal imaging system (Xenogen IVIS™ II system, Alameda) to analyze the mPEG–PEI–PLLA-IR800 diffusion and metabolism in 48 h.

Loading the mPEG–PEI–PLLA with paclitaxel

10 mg synthesized mPEG–PEI–PLLA copolymer and 3 mg paclitaxel (LC Laboratories) were dissolved and mixed in 5 mL acetone solution and sonicated for 10 min. Acetone was then removed by overnight evaporation with stir bar agitation. The mPEG–PEI–PLLA and PTX mixture was re-dissolved in 10 mL pure water. The solution was treated with 1000 rpm centrifuge for 1 min to remove unloaded PTX precipitate. High performance liquid chromatography (HPLC, Agilent Technologies 1200) was utilized to determine the PTX concentration of supernatant to calculate the loading amount.

PTX release in PBS

The release profile was determined in pH 7.4 PBS over a few days. Briefly, 50 μg mL^{-1} mPEG–PEI–PLLA–PTX micelles in PBS was loaded into slide-A-lyzer™ Dialysis Cassettes G2 (10 K, Thermo Fisher) and placed in 1.0 L PBS at 37 °C. Aliquots were taken out from the cassettes at predetermined times and mixed with equal volume of acetonitrile for HPLC analysis. The UV detector was set at 228 nm and peak areas were used to calculate PTX concentration.

Loading mPEG–PEI–PLLA–PTX with nitric oxide

The 10 mg synthesized mPEG–PEI–PLLA–PTX was dissolved in 5.0 mL acetic acid (Sigma-Aldrich) and bubbled with N_2 for 30 min. Excessive $NaNO_2$ (Sigma-Aldrich) was added into the solution and the mixture was kept in dark to load nitric oxide on the secondary amine of PEI. After 4 h reaction, 45 mL of degassed water was added to above solution, which was transferred into Millipore ultra-filtration tube (MW = 1000 Da, Merck Millipore) to remove the supernatant containing unreacted $NaNO_2$ by centrifugation at 4500 rpm for 15 min. After being washed with pure water for 5 times, the purified mPEG–PEI–PLLA–PTX–NO copolymer was redispersed in 10 mL N_2 degassed PBS (pH 7.4) for next experiment. Note that mPEG–PEI–PLLA–PTX–NO should be freshly made before use due to the spontaneous release of NO. Set the same amount of branched PEI 10 k to load NO as the control group.

NO release from mPEG–PEI–PLLA–NO

A classic commercial Griess assay (Promega) was utilized to monitor the NO release from mPEG–PEI–PLLA–PTX–NO micelles (PEI–NO as control). 100 μL of 200 μg mL^{-1} sample was mixed with 100 μL of sulfanilamide solution (1% sulfanilamide in 5% phosphoric acid) and was shaken at dark RT environment for 10 min. Then added 100 μL of the NED solution (0.1% *N*-1-napthylethylenediamine dihydrochloride in water) and was incubated at RT in dark for 10 min. Finally, the mixture was diluted with 200 μL pure water for UV-Vis measurement. mPEG–PEI–PLLA–PTX–NO micelles were kept at 37 °C or 4 °C in dark for several hours and monitored by Griess assay. The other two groups were treated with 365 nm UV or sonication for 5 min to detect NO release for comparison. A series of $NaNO_2$ standard samples (0.05–25 μM) were used to establish a standard curve for calculating the NO concentration.

Self-assembly of mPEG–PEI–PLLA–PTX–NO in water

2 mg mPEG–PEI–PLLA–PTX–NO compound was dissolved in 0.2 mL acetone by sonication, then 1 mL pure water was added dropwise and sonicated for 1 min. Then, acetone was removed by evaporation overnight, resulting in opalescent solution. Uranyl acetate (Sigma-Aldrich) was used to stain the mPEG–PEI–PLLA micelle to enhance contrast under TEM to characterize their morphology.

MTT assay of mPEG–PEI–PLLA–PTX–NO with anti-MDR cell OVCAR-8/ADR

OVCAR-8/ADR cells were seeded at a concentration of 5×10^5 in 96 wells plate, after incubation overnight, cells were treated with 100 μL of mPEG–PEI–PLLA–PTX–NO, mPEG–PEI–PLLA–PTX, mPEG–PEI–PLLA–NO, or mPEG–PEI–PLLA (each group contains about 100, 50, 25, 12.5, 6.25, 3.125, 0 μg mL^{-1} of mPEG–PEI–PLLA) RPMI 1640 medium (Corning Inc.) solution for each well. After incubation for 24 h, 3-(4,5-dimethylthiazol-2-yl)-2,5-diphenyltetrazolium (MTT, Sigma-Aldrich) assay was utilized to evaluate cell viability. Each datum point was represented as a mean ± standard deviation of at least 3 independent experiments.

Results and discussion

Synthesis of mPEG–PEI–PLLA copolymer

The azido functionality was introduced to PEI by reaction with azidoacetic acid. The synthesized PEI–N_3 was dissolved in DMSO-D_6 and characterized by ^{1}H NMR (Fig. S1†). The results indicated the characteristic peaks around 3.8 and 7.4 ppm. According to ^{1}H NMR, every 11 mmol PEI repeating units reacted with 1 mmol of azidoacetic acid.

The alkyne terminated PLLA was synthesized by ring-opening polymerization (ROP), which has been extensively utilized to synthesize various biocompatible and degradable polymers, such as polyesters, polypeptides, and polyphosphoesters.[28–30] Typically, stannous octoate is used as the catalyst for PLLA synthesis; however, metal residues may introduce some potential toxicity to biological systems. Therefore, biocompatible metal-free organocatalyst DBU was used. The propargyl alcohol was used as the initiator in order to introduce alkyne functional groups. The synthesized PLLA–alkyne was purified by precipitation from dichloromethane into hexane/ethyl ether mixture three times and vacuum-dried as

white powder with a yield of *ca.* 70%. The polymer was dissolved in $CDCl_3$ and characterized by ^1H NMR, observing characteristic PLLA peaks. L-Lactide monomers and 2-propynyl alcohol initiator were mixed at a ratio of 35 : 1. According to the ^1H NMR results (Fig. S2†), the polymer was determined to have 30 repeating units, which was similar to our target ratio. The gel permeation chromatography trace demonstrated that PLLA–alkyne had a peak retention time of around 26 min with unimodal distribution and low polydispersity (Fig. 2). Therefore, the PLLA with alkyne as one of the end groups was synthesized successfully.

The amphiphilic polymer mPEG–PEI–PLLA was synthesized by conjugating PLLA–alkyne and mPEG–alkyne to the PEI–azide backbone *via* the highly efficient copper(I)-catalyzed azide–alkyne Huisgen cycloaddition (CuAAC). The reaction mixture was stirred overnight and purified by dialysis against water for 2 days to remove copper and other impurities. During dialysis, the amphiphilic polymer self-assembled into nanoparticles spontaneously and no precipitation was found. Due to the strong hydrophobicity of PLLA, the formation of clear transparent nanoparticles demonstrated the successful conjugation of the three components. According to the mass of the raw materials, PEI containing 2 mmol amines and 0.15 mmol azido groups were conjugated with 0.035 mmol mPEG–alkyne (MW = 5000) and 0.035 mmol PLLA–alkyne. The characteristic peaks of all the three components, mPEG, PEI and PLLA, were found on the ^1H NMR spectrum (Fig. S3†).

Loading of paclitaxel and nitric oxide to mPEG–PEI–PLLA micelle

PTX was successfully loaded into the nanoparticles *via* co-assembly with the amphiphilic polymer in acetone/water mixture. Briefly, the mPEG–PEI–PLLA and PTX were mixed in acetone and water solution with vigorous stirring. After removal of acetone by overnight volatilization, the amphiphilic copolymer self-assembled into nanoparticles. During the co-assembly of PTX and polymer, unloaded PTX precipitated out and was removed by centrifugation. HPLC was utilized to detect PTX concentration in the supernatant. Under the optimized condition (H_2O : ACN = 1 : 1 solution, UV detection at 228 nm), PTX displayed a unimodal symmetric peak at 5.7 min (Fig. S4†). PTX standard curve was plotted with concentration ranging from 1.95 to 250 μg mL^{-1} (Fig. S5 and S6†). It was found that 0.5236 mg PTX was encapsulated into 10.0 mg of polymer, corresponding to a 5.0% loading.

The mPEG–PEI–PLLA–PTX was suspended in acetic acid. After adding excessive $NaNO_2$, the solution reacted violently and plenty of NO bubbles generated in the solution. The acetic acid solution turned light blue, which was caused by the production of N_2O_3. Because of the hydrophobic NO binding to the PEI secondary amines, the water solubility of mPEG–PEI–PLLA–PTX–NO decreased and the amphiphilic copolymer could self-assemble into micelle in PBS solution.

The above prepared nanoparticles were characterized by DLS and TEM (Fig. 3). The relatively dense PLLA provided some contrast and the nanoparticles could be observed directly (Fig. 3A), though not very clear. To enhance contrast, uranyl acetate was used (Fig. 3B). The circular shapes of these spots suggest that they were spherical micelles. On the other hand, the particles were found to have a hydrodynamic diameter of 137 nm, as measured by DLS (Fig. 3C). These mPEG–PEI–PLLA nanoparticles were positively charged with a zeta potential of *ca.* 45 mV (Fig. 3D), mainly because of the abundant amines along PEI backbones. The secondary amines are also excellent sites for NO binding. After NO loading, the zeta potential decreased to *ca.* 22 mV (Fig. 3D). The high level positive charge of PEI always contributes to high cytotoxicity. The decrease of particle zeta potential would lead to the increase of biocompatibility.

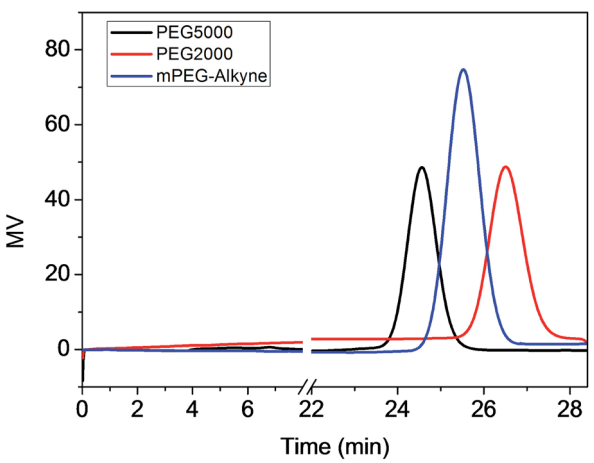

Fig. 2 The GPC results showed a significant peak of PLLA–alkyne in 25 min. The PEG5000 and PEG2000 were set as references.

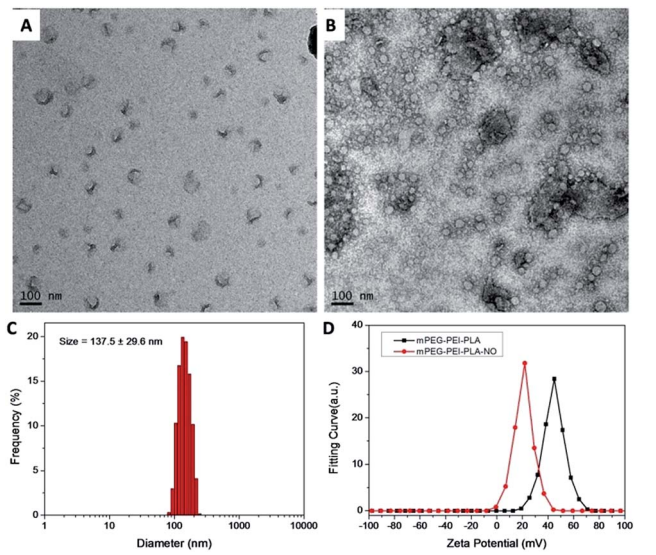

Fig. 3 TEM images of synthesized mPEG–PEI–PLLA–PTX–NO nanoparticles (A) and stained with uranyl acetate for enhanced contrast (B). (C) The size distribution of mPEG–PEI–PLLA–PTX–NO nanoparticles. (D) Zeta potentials of nanoparticles before and after NO loading.

The release of PTX and NO

The release of PTX from the nanoparticles was investigated in PBS at pH 7.4 by a dialysis method. Briefly, 3 mL of the mPEG–PEI–PLLA–PTX nanoparticle solution was injected into the dialysis cassettes and dialyzed against PBS for 7 days. The PTX concentration inside the cassettes was measured at predetermined times. It was found that PTX was released in a sustained manner after an initial burst release (Fig. 4A and S7†). After 7 days, most of the wrapped PTX had been released. The slow and controlled PTX release could potentially maintain a steady concentration in diseased tissue and reduced side effects.

The NO release profile from mPEG–PEI–PLLA–NO was investigated *via* Griess method (Fig. 4B and S8†). The 200 μg mL^{-1} prepared mPEG–PEI–PLLA–NO PBS solution was incubated in a 37 °C dark environment and monitored NO release. Another group of mPEG–PEI–PLLA–NO was incubated in 4 °C dark environment as control. A rapid release of NO was observed during the initial 8 h, followed by a much slower NO release in the 37 °C group, while a milder and longer lasting NO release was detected in the 4 °C dark condition. The 200 μg mL^{-1} mPEG–PEI–PLLA–NO could release NO spontaneously and the NO concentration increased to about 13 μM in 20 h under 37 °C dark conditions. The mPEG–PEI–PLLA–NO showed an extended NO release time than just PEI loaded NO (most NO released in 2 h). This result is similar to that reported by Nurhasni *et al.*[21] The PEI part of mPEG–PEI–PLLA copolymer was wrapped inside and surrounded by hydrophobic PLLA and amphiphilic PEG. After binding with NO, the hydrophobicity of the modified PEI increased which kept some cross-linked PEI–NO away from the solution and decreased their exposure to the oxidizing environment. The results indicated the copolymer of PEI with some biocompatible hydrophobic polymer may be a better strategy for NO molecules loading compared with PEI loaded NO. Furthermore, 2 groups of 200 μg mL^{-1} mPEG–PEI–PLLA–NO PBS solutions were treated with either UV exposure or sonication for 5 min. UV is found to be a more efficient method to trigger NO release from PEI–NO over sonication (Fig. S9†). The ultrasound is expected to become an *in vivo* application strategy for this nanomedicine.

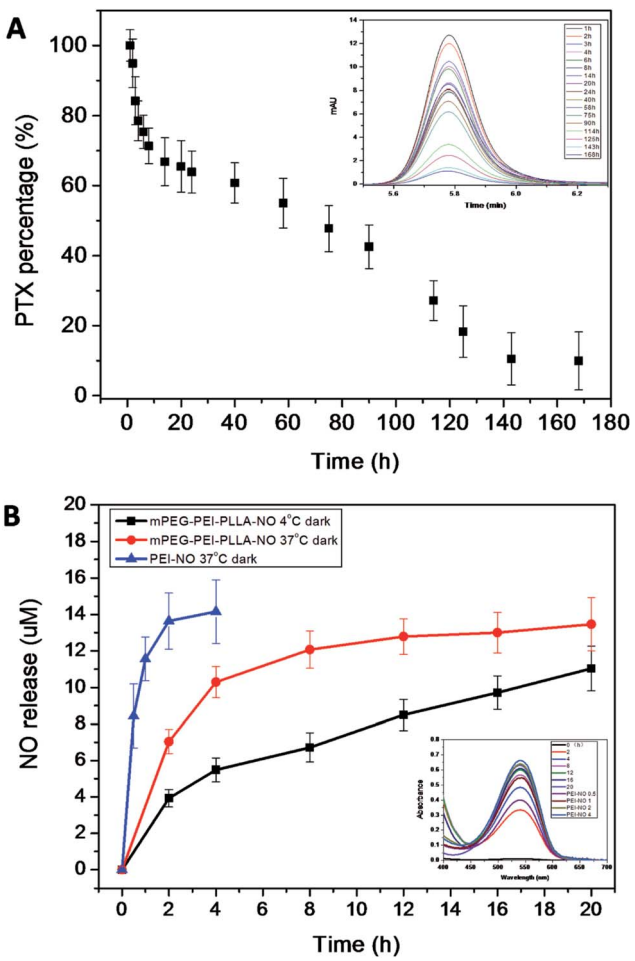

Fig. 4 (A) The release of PTX from mPEG–PEI–PLLA–PTX in pH 7.4 PBS. (B) NO loading and stability of mPEG–PEI–PLLA polymer *via* Griess method.

Biological evaluation of mPEG–PEI–PLLA–PTX–NO *in vitro* and *in vivo*

The cytotoxicity of mPEG–PEI–PLLA–PTX–NO micelles against MDR ovarian cancer cell line OVCAR-8/ADR was investigated by MTT assay (Fig. 5). The results showed that the mPEG–PEI–PLLA and the mPEG–PEI–PLLA–NO micelles presented a weak cytotoxicity against OVCAR-8/ADR cells at concentrations lower than 20 μg mL^{-1} (Fig. 5, black and blue line). The sample loaded with NO even had a better biocompatibility which may be caused by the decreased positive charges. The cytotoxicity of mPEG–PEI–PLLA–PTX–NO (IC50 = 32 μg mL^{-1}) and mPEG–PEI–PLLA–PTX sample (IC50 = 44 μg mL^{-1}) both increased in comparison with mPEG–PEI–PLLA (IC50 = 70 μg mL^{-1}) and mPEG–PEI–PLLA–NO (IC50 = 82 μg mL^{-1}) groups (Fig. 5, red and pink line). The mPEG–PEI–PLLA–PTX–NO generated the

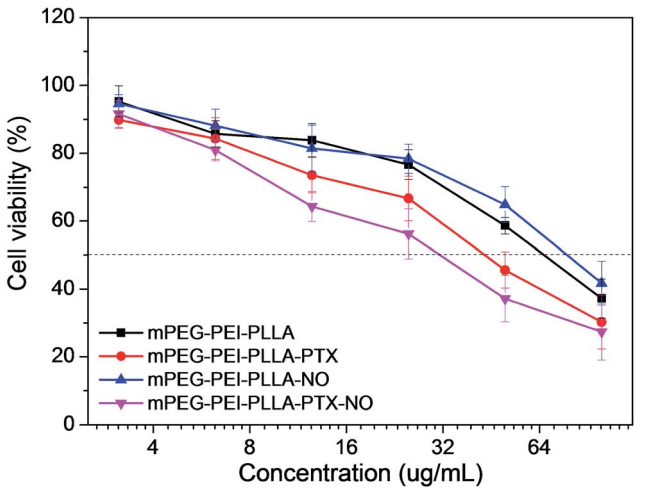

Fig. 5 The cytotoxicity of mPEG–PEI–PLLA–PTX–NO micelles against MDR ovarian cancer cell line OVCAR-8/ADR, measured by MTT assay. Each datum point was represented as a mean ± standard deviation of at least 3 independent experiments.

highest toxicity, higher than mPEG–PEI–PLLA–NO. The spontaneous release of NO from PEI–NO may reverse the MDR and made the PTX achieve higher cytotoxicity to this MDR cell line. After wrapped with PLLA and PEG, the prepared nanoparticles may have lower cytotoxicity compared to PEI. The synergistic effect of paclitaxel and NO towards cancer therapy was also demonstrated by other investigators. Jia *et al.* demonstrated that the effect of nitric oxide on cytotoxicity of taxol should be mediated *via* the increased influx of taxol by NO into intracellular compartments, though NO-induced cytotoxicity could be possible.[31] Graham *et al.* systemically studied the mechanism of nitric oxide reversing drug resistance in tumor. They employed glyceryl trinitrate and isosorbide dinitrate as NO donor and successfully attenuated the hypoxia-induced resistance to doxorubicin and paclitaxel. They concluded that the inhibition of various components of the NO signaling pathway increased resistance to chemotherapeutic agent, whereas activation with 8-bromo-cGMP which was a downstream signal molecule in NO pathway could attenuate this process. It reminds endogenous NO signaling was able to effect the hypoxia-induced drug resistance and reactivation of NO signaling pathway is a hopeful novel strategy to enhance chemotherapy.[32]

In order to investigate the biological effects and distribution of mPEG–PEI–PLLA micelles *in vitro* and *in vivo*, a near infrared fluorescent dye IR-800 with negative charges was connected to the positive charged mPEG–PEI–PLLA by amidation chemistry (Fig. S10†) between primary amines of PEI and NHS ester of IR-800. After reaction, unreacted dyes and other small molecules were removed by dialysis, followed by lyophilization, yielding a blue-green copolymer powder. The characteristic peaks of IR-800 were detected in the water solution as shown by UV-Vis spectrum. There was a high scattering background in UV-Vis scan as a result of the self-assembly of amphiphilic mPEG–PEI–PLLA-IR800 into micelle in water.

Cellular uptake of nanoparticles was investigated in multidrug resistance cell line OVCAR-8/ADR *via* fluorescence imaging. After incubation for 2 hours, OVCAR-8/ADR seeded slides were observed live by fluorescent microscopy. The mPEG–PEI–PLLA-IR800 group was found to have significant fluorescent signals in cytoplasm through CY 5.0 dye optical channel (Fig. 6A and B). But in the control group of free IR-800, there was almost no fluorescent signal observed under the same observation condition (Fig. 6C and D). The results showed that the positive charged carriers was much more efficient to cross negative charged cell membrane rather than the just negative charged IR-800 dye. It is expected that the positive charged nanoparticle could transport NO and PTX into cells efficiently. The "proton sponge effect" introduced by PEI could help the nanoparticle and encapsulated PTX to escape into the cytoplasm to achieve the synergistic therapy of NO and PTX.[33]

The nanoparticles were also injected into tumor *via* intra tumor injection. After 48 h, there was still strong IR-800 fluorescent signal observed in tumor tissues (Fig. 6E, F and S11†). The obvious contrast suggested high concentration of these nanoparticle remained in the tumor, which might be caused by the positive charged nanoparticles through electrostatic adherence and higher cellular uptake by tumor cells. The longer

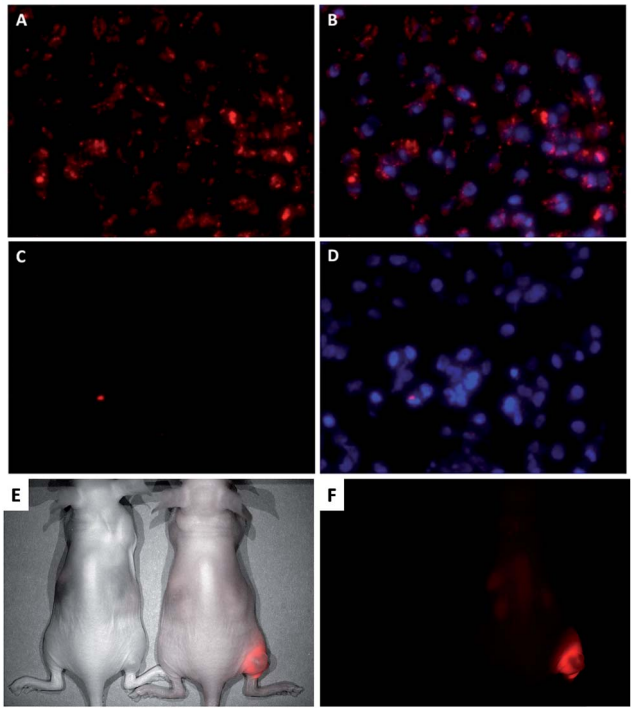

Fig. 6 After incubation for 2 hours, OVCAR-8/ADR seeded slides were observed by fluorescent microscopy. The mPEG–PEI–PLLA-IR800 group was found to have significant fluorescent signals in cytoplasm through CY 5.0 dye optical channel (A and B). In the free IR-800 control group, there was almost no fluorescent signal observed under the same observation condition (C and D). Red: Cy 5.0 channel; blue: DAPI channel. *In vivo* experiment indicated that there was still strong IR-800 fluorescent signal observed in tumor tissues (F: whole body fluorescent channel imaging, E: merge with bright-field image) 48 h after intratumor injection. The body fluorescence signal of the experimental mice was also stronger than that of the control mice and some fluorescent light emitted from intra-abdominal was also found. The left mice was treated with mPEG–PEI–PLLA and the right mice was treated with mPEG–PEI–PLLA-IR800.

retention allows their payload continually released inside the tumor tissues. The body fluorescence signal of the experimental mice was also stronger than that of the control mice, which indicated that the nanomaterials flowed over body through bloodstream. Some fluorescent light emitted from intra-abdominal was also found, suggesting a relative higher uptake in the liver and spleen. The liver and spleen, as part of the mononuclear-phagocytic cell system, functioned as a filter for toxins and to remove extraneous foreign matter in blood.[34] The *in vivo* fluorescence imaging results of mPEG–PEI–PLLA-IR800 showed that mPEG–PEI–PLLA-IR800 nanoparticles were similar to most nanoparticles which could be phagocytized by monocytes/macrophages after being identified by monocyte–macrophage system, and then be cleared out body through the liver and spleen metabolism.

Conclusions

In this research, polyethylenimine (PEI) with abundant secondary amine for NO binding was modified with azido

functional groups and reacted with alkyne-terminated mPEG and PLLA polymer to afford a three-segment amphiphilic copolymer. The hydrophobic PLLA encapsulated hydrophobic drugs paclitaxel (PTX) while the secondary amine of PEI was to load nitric oxide. This multifunctional copolymer was resuspended readily in water and self-assembled into micelles. The mPEG–PEI–PLLA–PTX–NO nanomedicine was able to release NO spontaneously under physiological conditions and enhance the *in vitro* cytotoxicity for PTX and NO synergistic treatment. These nanoparticles were also found to remain in the tumor for more than 48 hour, demonstrating potential application in the treatment of MDR ovarian cancer.

Acknowledgements

We thank the financial support from the Intramural Research Program, National Institute of Biomedical Imaging and Bioengineering, National Institutes of Health, the National Key Program for Developing Basic Research of China (2014CB744501), the NSFC (61271056, 61471168, and 61527806), and the State Scholarship Fund from China Scholarship Council (201406090085).

Notes and references

1 A. Persidis, *Nat. Biotechnol.*, 1999, **17**, 94–95.
2 F. Grandjean, L. Brémaud, M. Verdier, J. Robert and M.-H. Ratinaud, *Anti-Cancer Drugs*, 2001, **12**, 247–258.
3 J. Kopecka, I. Campia, D. Brusa, S. Doublier, L. Matera, D. Ghigo, A. Bosia and C. Riganti, *J. Cell. Mol. Med.*, 2011, **15**, 1492–1504.
4 Y. Ogiso, A. Tomida, S. Lei, S. Ōura and T. Tsuruo, *Cancer Res.*, 2000, **60**, 2429–2434.
5 P. W. Vaupel, *Klin. Padiatr.*, 1996, **209**, 243–249.
6 B. A. Teicher, *Cancer Metastasis Rev.*, 1994, **13**, 139–168.
7 A. W. Carpenter and M. H. Schoenfisch, *Chem. Soc. Rev.*, 2012, **41**, 3742–3752.
8 D. Fukumura, S. Kashiwagi and R. K. Jain, *Nat. Rev. Cancer*, 2006, **6**, 521–534.
9 E. M. Hetrick and M. H. Schoenfisch, *Chem. Soc. Rev.*, 2006, **35**, 780–789.
10 S. Mocellin, V. Bronte and D. Nitti, *Med. Res. Rev.*, 2007, **27**, 317–352.
11 J. Fan, N. He, Q. He, Y. Liu, Y. Ma, X. Fu, Y. Liu, P. Huang and X. Chen, *Nanoscale*, 2015, **7**, 20055–20062.
12 C. Muir, M. Adams and C. Graham, *Breast Cancer Res. Treat.*, 2006, **96**, 169–176.
13 Z. Ren, X. Gu, B. Lu, Y. Chen, G. Chen, J. Feng, J. Lin, Y. Zhang and H. Peng, *J. Cell. Mol. Med.*, 2016, **20**, 1095–1105.
14 V. R. Prasad, G. D. Reddy, I. Kathmann, M. Amareswararao and G. Peters, *Bioorg. Chem.*, 2016, **64**, 51–58.
15 X. Zhang, G. Tian, W. Yin, L. Wang, X. Zheng, L. Yan, J. Li, H. Su, C. Chen and Z. Gu, *Adv. Funct. Mater.*, 2015, **25**, 3049–3056.
16 V. Rapozzi, E. Della Pietra and B. Bonavida, *Redox Biol.*, 2015, **6**, 311–317.
17 H. Pelicano, D. Carney and P. Huang, *Drug Resist. Updates*, 2004, **7**, 97–110.
18 D. A. Wink, K. M. Miranda, M. G. Espey, R. M. Pluta, S. J. Hewett, C. Colton, M. Vitek, M. Feelisch and M. B. Grisham, *Antioxid. Redox Signaling*, 2001, **3**, 203–213.
19 M. F. Chung, H. Y. Liu, K. J. Lin, W. T. Chia and H. W. Sung, *Angew. Chem.*, 2015, **127**, 10028–10031.
20 J. Fan, Q. He, Y. Liu, F. Zhang, X. Yang, Z. Wang, N. Lu, W. Fan, L.-S. Lin and G. Niu, *ACS Appl. Mater. Interfaces*, 2016, **8**, 13804–13811.
21 H. Nurhasni, J. Cao, M. Choi, I. Kim, B. L. Lee, Y. Jung and J.-W. Yoo, *Int. J. Nanomed.*, 2015, **10**, 3065.
22 J. Kim, Y. Lee, K. Singha, H. W. Kim, J. H. Shin, S. Jo, D.-K. Han and W. J. Kim, *Bioconjugate Chem.*, 2011, **22**, 1031–1038.
23 Y. Wan, Y. Zheng, X. Song, X. Hu, S. Liu, T. Tong and X. Jing, *J. Biomater. Sci., Polym. Ed.*, 2011, **22**, 1131–1146.
24 B. Woerle, C. Hanke and G. Sattler, *J. Drugs Dermatol.*, 2003, **3**, 385–389.
25 K. A. Athanasiou, G. G. Niederauer and C. M. Agrawal, *Biomaterials*, 1996, **17**, 93–102.
26 W. Liu, J. Wei and Y. Chen, *New J. Chem.*, 2014, **38**, 6223–6229.
27 F. Zhang, S. Zhang, S. F. Pollack, R. Li, A. M. Gonzalez, J. Fan, J. Zou, S. E. Leininger, A. Pavía-Sanders and R. Johnson, *J. Am. Chem. Soc.*, 2015, **137**, 2056–2066.
28 X. He, J. Fan, F. Zhang, R. Li, K. A. Pollack, J. E. Raymond, J. Zou and K. L. Wooley, *J. Mater. Chem. B*, 2014, **2**, 8123–8130.
29 A. Li, H. P. Luehmann, G. Sun, S. Samarajeewa, J. Zou, S. Zhang, F. Zhang, M. J. Welch, Y. Liu and K. L. Wooley, *ACS Nano*, 2012, **6**, 8970–8982.
30 Y. Shen, S. Zhang, F. Zhang, A. Loftis, A. Pavía-Sanders, J. Zou, J. Fan, J. S. A. Taylor and K. L. Wooley, *Adv. Mater.*, 2013, **25**, 5609–5614.
31 L. Jia, J. Schweizer, Y. Wang, C. Cerna, H. Wong and M. Revilla, *Biochem. Pharmacol.*, 2003, **66**, 2193–2199.
32 L. J. Frederiksen, R. Sullivan, L. R. Maxwell, S. K. Macdonald-Goodfellow, M. A. Adams, B. M. Bennett, D. R. Siemens and C. H. Graham, *Clin. Cancer Res.*, 2007, **13**, 2199–2206.
33 A. E. Nel, L. Mädler, D. Velegol, T. Xia, E. M. Hoek, P. Somasundaran, F. Klaessig, V. Castranova and M. Thompson, *Nat. Mater.*, 2009, **8**, 543–557.
34 K. M. Tsoi, S. A. Macparland, X. Z. Ma, V. N. Spetzler, J. Echeverri, B. Ouyang, S. M. Fadel, E. A. Sykes, N. Goldaracena and J. M. Kaths, *Nat. Mater.*, 2016, **15**, 1212–1221.